Electronic Supplementary Material (ESI) for Polymer Chemistry.
This journal is © The Royal Society of Chemistry 2016

**Supporting Information**

# Thermal Stability Enhancement of Hydrogen Bonded Semicrystalline Thermoplastics Achieved by Combination of Aramid Chemistry and Supramolecular Chemistry

*Mikihiro Hayashi*[†], *François Tournilhac*[*]

Matière Molle et Chimie (UMR 7167 CNRS-ESPCI Paris), PSL Research University, 10 rue Vauquelin, 75005 Paris, France

Present address

† M.H. (Prof. Tokita group, Department of Chemical Science and Engineering, School of Materials and Chemical Technology, Tokyo Institute of Technology, Ookayama 2-12-1, Meguro-ku, Tokyo 152-8552, Japan)

**1. Synthesis procedure of supramolecular compounds**

**2. $^1$HNMR analysis**

**3. FT-IR spectra**

**4. Self-association in solution**

**5. TGA data of the end capping molecules**

**6. DSC thermograms**

**7. Isothermal TGA data of the final compounds**

**8. Variable temperature FT-IR measurements on compound 8 and compound 6**

**9. Plots of $\ln\eta$ as a function of inverse temperatures**

**10. Tensile data of compound 6**

**11. References**

1. **Synthesis procedure of supramolecular compounds**

1-1. Synthesis of compound **6**

Scheme S1. Note: Pripol 1009 is a derivative of natural fatty acids, mainly composed of alicyclic dicarboxylic acids. The idealized scheme presented below is only one possible chemical structures, among others.

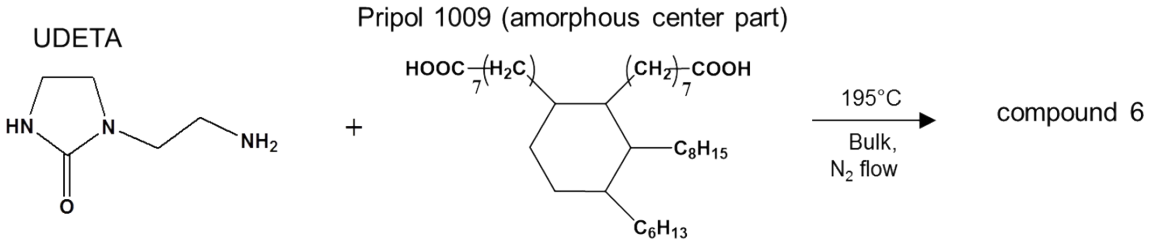


The synthesis was made as shown in Scheme S1. In a 100 mL three-necked flask equipped with a gas inlet and a magnetic stirring bar, Pripol (6 g, 21 mmol of COOH group) was heated at 160 °C with an oil bath. UDETA (2.99 g, 23.1 mmol of $NH_2$ group) was added and the mixture was homogenized. The temperature of the oil bath was raised to 195 °C. The condensation reaction was conducted in bulk for 90 min under $N_2$ flow.

1-2. Synthesis of compound **8**

Compound **8** was prepared according to Scheme S2.

Scheme S2.

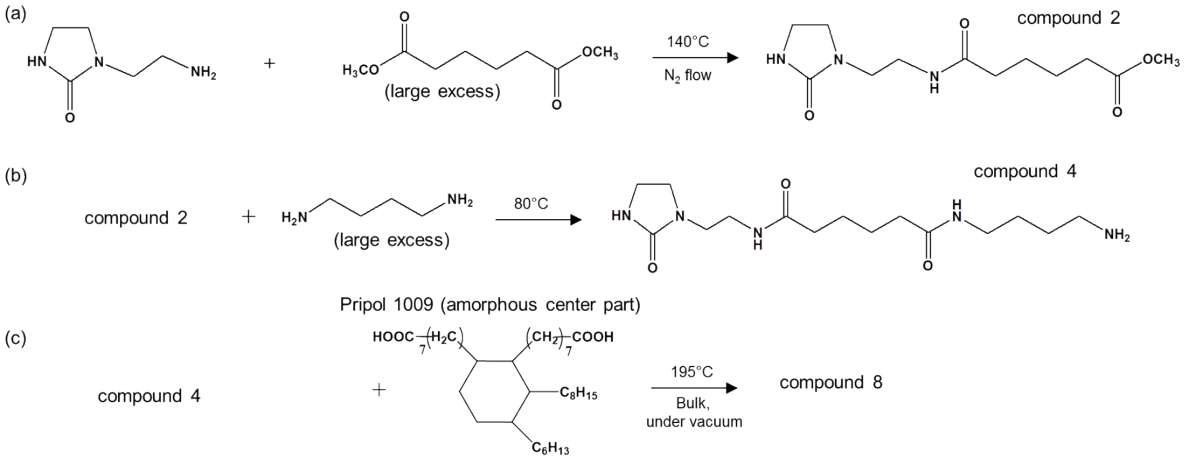


1-2-1. Synthesis of compound **2**.

The synthesis was performed as already reported. [1]

1-2-2. Synthesis of compound **4**.

Compound **4** was synthesized from compound **2**: 1,4-diaminobutane (64 g, 1.5 mol of $NH_2$ group) was put into the three-neck flask fitted with a stirring bar and a reflux condenser. Compound **2** (10 g, 37 mmol of methoxy group) was then added to the flask and the resulting mixture was homogenized at 80 °C. The reactive mixture was kept at 80 °C for the first 3h, and then the temperature was increased to 140 °C and kept for further 1 hour to complete the reaction. After the reaction, unreacted excess amine molecule was removed by precipitation of the reaction mixture into toluene. Further purification was conducted by selective washing with chloroform at 60 °C.

1-2-3. Synthesis of compound **8**.

In a 100 mL three-necked flask equipped with a vacuum inlet and a magnetic stirring bar, Pripol 1009 (3.17 g, 11.1 mmol of COOH group) was heated at 195 °C with an oil bath. Then, the end capping molecule, compound **4** (4 g, 12.2 mmol of $NH_2$ group), was added and the mixture was homogenized. The condensation reaction was conducted in bulk at 195 °C for 90 min under reduced pressure.

1-3. Synthesis of compound **9**

Compound **9** was prepared according to Scheme S3.

Scheme S3.

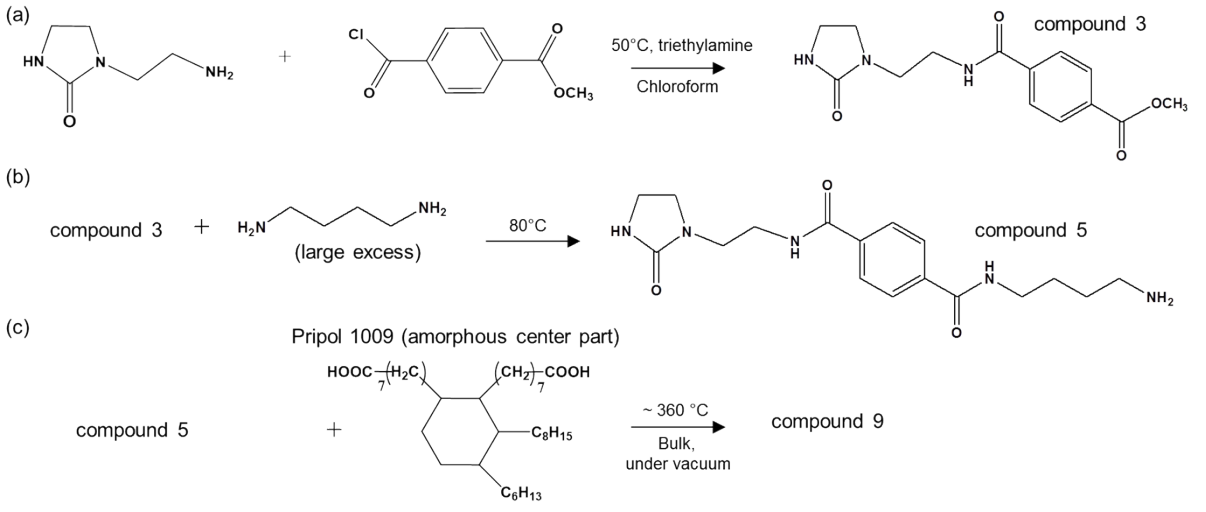

1-3-1. Synthesis of compound **3**.

In a 500 mL three necked flask equipped with a magnetic bar and a reflux condenser, 7.8 g UDETA (60.4 mmol of $NH_2$) was dissolved in chloroform (200 mL) at 50 °C. Then, triethylamime (25 g) was added. A solution of 12 g MCCB (60.4 mmol of COCl) in 150 mL of chloroform was added dropwise to the previous UDETA solution. The resulting mixture was stirred at 50 °C for 5 hours. After evaporation of all volatile materials, the residue was redissolved in chloroform, and the salts generated by the reaction were removed by washing with brine. After washing with clear water, drying over magnesium sulphate, compound **3** was isolated by evaporation of the solvent and then further purified by recrystallization from a methyl acetate solution.

1-3-2. Synthesis of compound **5**

In a 100 mL three-necked flask equipped with a magnetic bar and a reflux condenser, 48 g of 1,4-diaminobutane (1.1 mol of $NH_2$) were placed, together with 8 g of compound **3** (27 mmol of methoxy group). The mixture was homogenized by stirring at 80 °C. The reaction was kept at 80 °C for the first 3h, and then the temperature was increased to 140 °C and kept for further 1 hour to complete the reaction. After the reaction, unreacted excess amine molecule was removed by reprecipitation of the reaction mixture into toluene. The product obtained after evaporation of toluene was further purified by selective washing with ethanol at 70 °C.

1-3-3. Synthesis of compound **9**

A 50 mL flask, fitted with a vacuum connector, a magnetic stirring bar and containing Pripol 1009 (3 g, 10.5 mmol of COOH groups) was placed into a sand bath, preheated at 300 °C to ensure a starting temperature above 180 °C. Then, the end-capping molecule, compound **5** (4 g, 11.5 mmol of $NH_2$ group), was added. The mixture was carefully put under vacuum and stirred. A homogeneous reaction mixture was rapidly obtained, and formation of gas bubbles was observed, indicating water evolution, taken as a criterion of reaction progress. Stirring was continued for 90 minutes while the temperature of the sand bath was gradually increased (up to 370 °C) in order to permit stirring throught the reaction. At the end of gas evolution, the glass flask was pulled out from the sand bath and cooled down under vacuum.

During cooling, crystallization was observed, resulting in a non-adhesive plastic-like material that easily unmolded from the reaction flask.

## 2. $^1$H-NMR analysis

$^1$H-NMR spectra at each synthesis step are shown in Figure S1 to S3 for the synthesis of the supramolecular polymers compound **9**, compound **8**, and compound **6**, respectively. For each compound, the spectra in the high ppm region and in the low ppm region are presented in (a) and (b) panels. The measurement set-up and condition are described in the experimental section of the main text. Attribution of each signal and comparison between experimental integral values and expected integral values are provided in Tables S1 to S3, where the signal codes in the tables correspond to the same codes in the corresponding spectra. A peak from $CD_3OD$ at 3.35 ppm was used as a reference position.

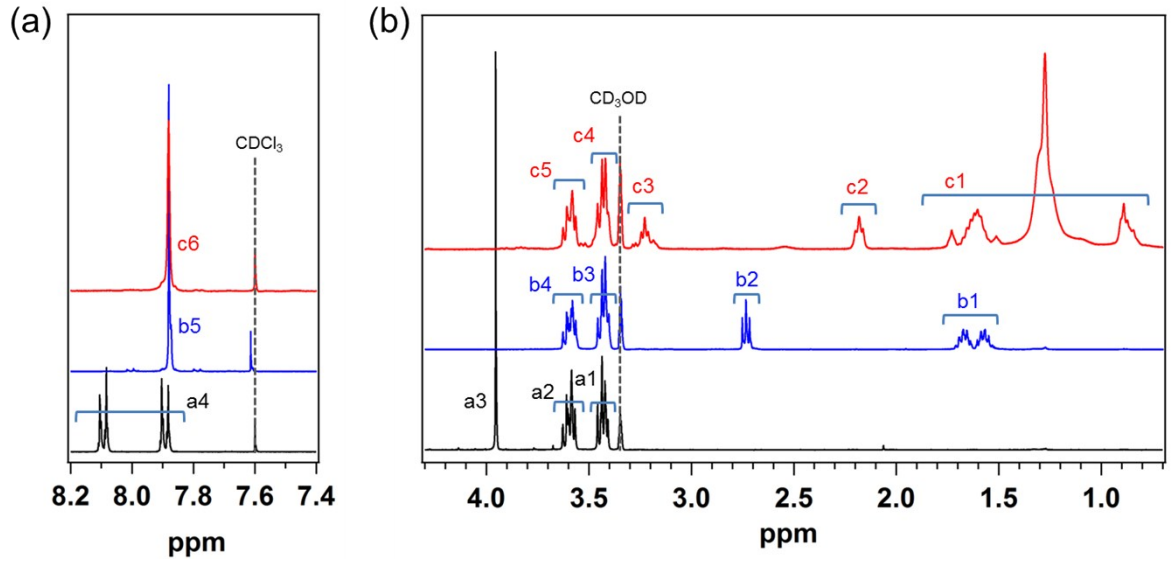


Figure S1. NMR spectra of compound **3** (black), compound **5** (blue), and compound **9** (red) in the high ppm region (a) and in the low ppm region (b). Peak assignment and integral values are provided in Table S1. The solvent used was mixture of $CDCl_3$ / $CD_3OD$ (1/1 vol%).

Table S1. Attribution of signals and integral values for compound **3** (top), compound **5** (middle), and compound **9** (bottom).

| | σ (ppm) | attribution | integral found | expected |
|---|---|---|---|---|
| a1 | 3.41 – 3.46 | N-C<u>H</u>$_2$ | 4.1 | 4 |
| a2 | 3.57 – 3.63 | N-C<u>H</u>$_2$ (imidazolidone) | 4.1 | 4 |
| a3 | 3.95 | OC<u>H</u>$_3$ | 3 | 3 |
| a4 | 7.88 – 8.11(double doublet) | <u>H</u>C=C (aromatic) | 4 | 4 |

| | σ (ppm) | attribution | integral found | expected |
|---|---|---|---|---|
| b1 | 1.55-1.66 | C<u>H</u>$_2$-CH$_2$-N | 4.1 | 4 |
| b2 | 2.72 (triplet) | C<u>H</u>$_2$-NH2, | 2 | 2 |
| b3 | 3.41 | N-C<u>H</u>$_2$, C<u>H</u>$_2$-NH-CO-Ph | 6 | 6 |
| b4 | 3. 57 | N-C<u>H</u>$_2$ (imidazolidone) | 4.1 | 4 |
| b5 | 7.87 (singlet) | <u>H</u>C=C (aromatic) | 3.9 | 4 |

| | σ (ppm) | attribution | integral found | expected |
|---|---|---|---|---|
| c1 | 0.89 | C<u>H</u>$_3$ | 75 | 62 – 70* |
| | 1.28 | C<u>H</u>$_2$ (Pripol) | | |
| | 1.49-1.7 | C<u>H</u>$_2$-CH$_2$-N,<br>C<u>H</u>$_2$-CH$_2$-CONH | | |
| | 2.54 | allylic C<u>H</u> | | |
| c2 | 2.18 | C<u>H</u>$_2$-CO-NH | 4 | 4 |
| c3 | 3.23 | C<u>H</u>$_2$-NH-CO-alkyl | 4.2 | 4 |
| c4 | 3.42 | N-C<u>H</u>$_2$, C<u>H</u>$_2$-NH-CO-Ph | 11.6 | 12 |
| c5 | 3.58 | N-C<u>H</u>$_2$ (imidazolidone) | 8 | 8 |
| c6 | 7.88 | <u>H</u>C=C (aromatic) | 7.8 | 8 |

* depending on residual unsaturation

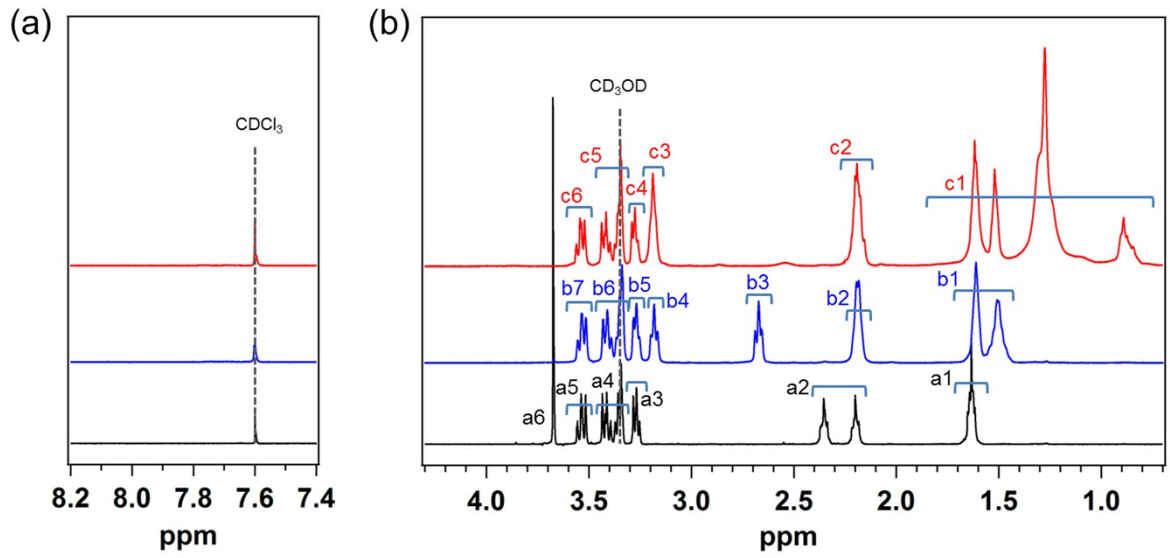


Figure S2. NMR spectra of compound **2** (black), compound **4** (blue), and compound **8** (red) in the high ppm region (a) and in the low ppm region (b). Peak assignment and integral values are provided in Table S2. The solvent used was mixture of $CDCl_3$ / $CD_3OD$ (1/1 vol%).

Table S2. Attribution of signals and integral values for compound **2** (top), compound **4** (middle), and compound **8** (bottom).

| | σ (ppm) | attribution | integral found | expected |
|---|---|---|---|---|
| a1 | 1.63 | $C\underline{H_2}$-$CH_2$-CO | 4.2 | 4 |
| a2 | 2.20, 2.53 | $C\underline{H_2}$-CO-NH<br>$C\underline{H_2}$-$COOCH_3$ | 4.2 | 4 |
| a3 | 3.27 | N-$C\underline{H_2}$ | 2 | 2 |
| a4 | 3.34-3.41 | N-$C\underline{H_2}$, N-$C\underline{H_2}$ (imidazolidone)<br>solvent | 4.96 | 4 + solvent |
| a5 | 3.54 | N-$C\underline{H_2}$ (imidazolidone) | 2.1 | 2 |
| a6 | 3.68 | $OC\underline{H_3}$ | 3 | 3 |

| | σ (ppm) | attribution | integral found | expected |
|---|---|---|---|---|
| b1 | 1.51, 1.61 | $C\underline{H_2}$-$CH_2$-NH<br>$C\underline{H_2}$-$CH_2$-CO | 7.9 | 8 |
| b2 | 2.18 | $C\underline{H_2}$-CO-NH | 3.9 | 4 |
| b3 | 2.67 | $C\underline{H_2}$-$NH_2$ | 1.9 | 2 |
| b4 | 3.18 | $C\underline{H_2}$-NH-CO | 1.9 | 2 |
| b5 | 3.27 | N-$C\underline{H_2}$ | 2 | 2 |
| b6 | 3.34 – 3.41 | N-$C\underline{H_2}$, N-$C\underline{H_2}$ (imidazolidone)<br>solvent | 5 | 4 + solvent |
| b7 | 3.54 | N-$C\underline{H_2}$ (imidazolidone) | 2 | 2 |

| | σ (ppm) | attribution | integral found | expected |
|---|---|---|---|---|
| c1 | 0.89 | $C\underline{H_3}$ | 75 | 70 – 78* |
| | 1.28 | $C\underline{H_2}$ (Pripol) | | |
| | 1.52 -1.62 | $C\underline{H_2}$-$CH_2$-N,<br>$C\underline{H_2}$-$CH_2$-CONH | | |
| | 2.54 | allylic C$\underline{H}$ | | |
| c2 | 2.19 | $C\underline{H_2}$-CO-NH | 11.9 | 12 |
| c3 | 3.19 | $C\underline{H_2}$-NH-CO-alkyl | 7.6 | 8 |
| c4 | 3.28 | N-$C\underline{H_2}$ | 4 | 4 |
| c5 | 3.35 – 3.42 | N-$C\underline{H_2}$, N-$C\underline{H_2}$ (imidazolidone) | 10.9 | 8+solvent |
| c6 | 3.54 | N-$C\underline{H_2}$ (imidazolidone) | 4.1 | 4 |

* depending on residual unsaturation

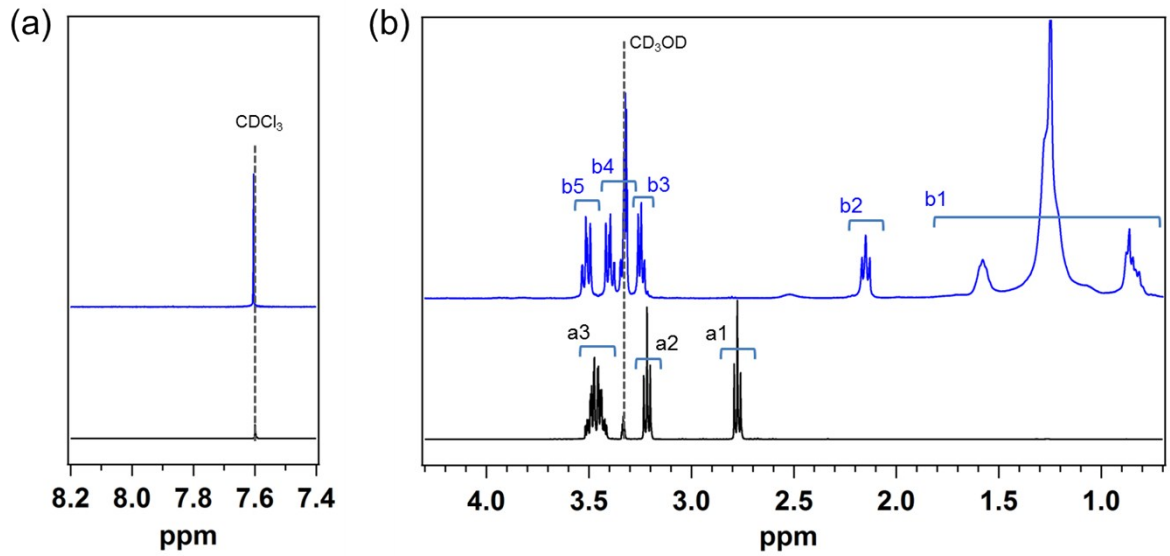


Figure S3. NMR spectra of compound **1** (black) and compound **6** (blue) in the high ppm region (a) and in the low ppm region (b). Peak assignment and integral values are provided in Table S3. The solvent used was mixture of $CDCl_3$ / $CD_3OD$ (1/1 vol%).

Table S3. Attribution of signals and integral values for compound **1** (top) and compound **6** (bottom).

| | σ (ppm) | attribution | integral found | expected |
|---|---|---|---|---|
| a1 | 2.78 | $C\underline{H_2}$-NH2 | 2 | 2 |
| a2 | 3.22 | N-$C\underline{H_2}$ | 2 | 2 |
| a3 | 3.47 | N-$C\underline{H_2}$ (imidazolidone) | 4 | 4 |

| | σ (ppm) | attribution | integral found | expected |
|---|---|---|---|---|
| b1 | 0.89 | $C\underline{H_3}$ | 62 | 54 – 62* |
| | 1.28 | $C\underline{H_2}$ (Pripol) | | |
| | 1.61 | $C\underline{H_2}$-$CH_2$-CO | | |
| | 2.54 | allylic C$\underline{H}$ | | |
| b2 | 2.18 | $C\underline{H_2}$-CO-NH | 4.1 | 4 |
| b3 | 3.27 | N-$C\underline{H_2}$ | 4.1 | 4 |
| b4 | 3.35 – 3.42 | N-$C\underline{H_2}$<br>N-$C\underline{H_2}$ (imidazolidone) | 10.3 | 8+solvent |
| b5 | 3.54 | N-$C\underline{H_2}$ (imidazolidone) | 4 | 4 |

* depending on residual unsaturation

**Comparison of NMR spectra of compound 6 and compound 9**

Comparison of NMR spectra of compound **6** (black) and compound **9** (red) is provided in Figure S4(a). The small peaks observed in the spectrum of compound **9** at around 3.3 ppm and 3.55 ppm, which actually cannot be assigned to any protons of the target molecule, are clearly overlapped with the distinctive peaks observed in the spectrum of compound **6** as indicated with blue arrows. Considering that the condensation of compound **5** and Pripol 1009 was carried out at high temperature, the transamidation side-reaction is likely to take place,[2] giving rise to a small quantity of end-capping groups where UDETA is linked directly to the aliphatic acyl group, as in compound **6**. This consideration is consistent with the overlapping of the unassigned small peaks in the spectrum of compound **9** with those of compound **6**. The event of transamidation side-reaction in the reaction of compound **5** and Pripol 1009 is illustrated in Figure S4(b).

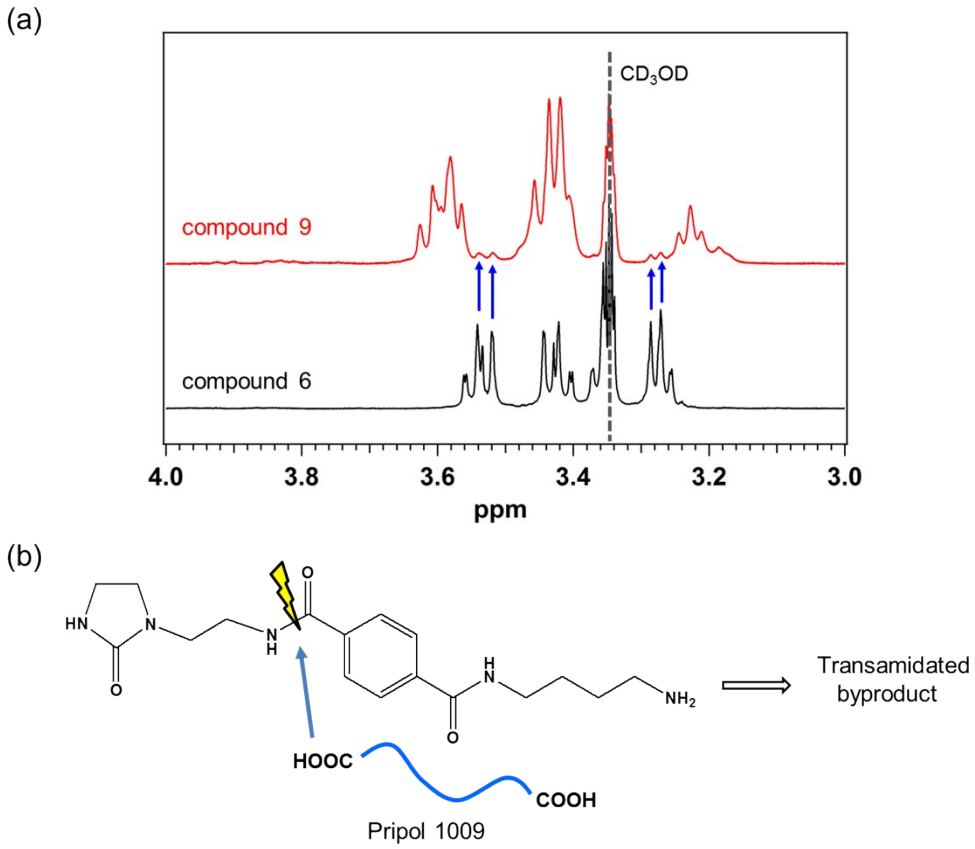


Figure S4. (a) Comparison of NMR spectra of compound **6** (black) and compound **9** (red). The peak from $CD_3OD$ is used as a reference. (b) Expected result of transamidation caused in the reaction of compound **5** and Pripol 1009 at high temperature.

### 3. FT-IR spectra

FT-IR spectra of the final compounds, that is, compound **9**, compound **8**, and compound **6** are shown in Figure S5. Experimental set-up and measurement conditions are described in the experimental part of the main text. Assignments of characteristic peaks are also provided in the spectra, where abbreviations σ and ν are used for bending and stretching vibration modes, respectively.

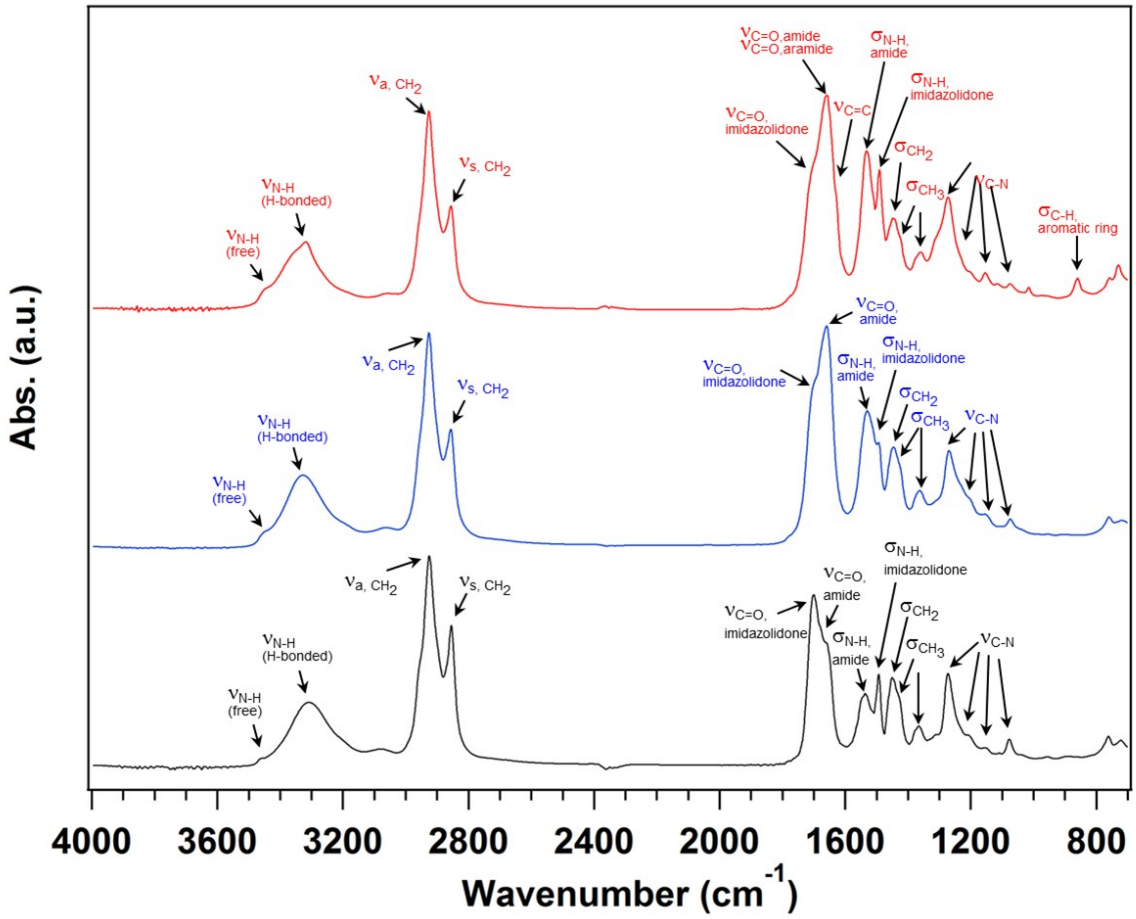


Figure S5. FT-IR spectra for compound **9** (red), compound **8** (blue), and (c) compound **6** (black).

## 4. Self-association in solution

The effects of supramolecular association of end groups have been investigated by $^1$H NMR. In order to cover a broad range of concentrations, the model compound **S1** was synthesized as follows and studied:

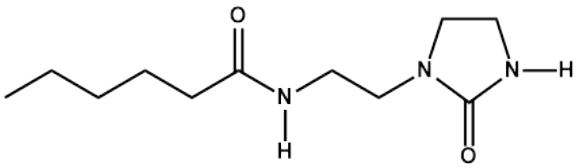

Preparation: Hexanoic acid (23.45g, 0.2 mol) is condensed with UDETA (26g, 0,2 mol) at 170 °C under a nitrogen atmosphere for 19h. After recrystallization (twice from toluene), compound S1 is obtained as a white solid with melting point Tm = 102 °C (max. endotherm). Spectroscopic analyses are consistent with the molecular structure of compound **S1**.

$^1$H NMR spectra of compound **S1** were recorded at various concentrations using a Bruker Avance 400 spectrometer and a $CCl_4/C_6D_6$ (90:10 v/v) mixture as the solvent.
When increasing the concentration, the $^1$H chemical shifts of both amide and imidazolidone H-bonded protons are shifted towards higher values. In the conditions of rapid exchange, the apparent chemical shift of a partially bonded assembly obeys the classical equation: [3]

$$\delta = \delta_d + (\delta_d - \delta_m)\frac{1-\sqrt{1+8Kc}}{4Kc} \quad \text{(S1)}$$

where $\delta$ is the measured averaged chemical shift, $K$ is the association constant, $c$ is the concentration, $\delta_m$ and $\delta_d$ are boundary chemical shift values for the monomer and dimer species, respectively.

The value of the dimerization constant of compound **S1** at 298 K was obtained from the concentration dependence of the $^1$H chemical shift of the N-H protons of imidazolidone and amide functions in the $10^{-3}$ to $10^{-2}$ L·mol$^{-1}$ range (Table S4). The fit of data using equation (S1) leads to two different association constants $K_A$ and $K_I$ for the amide and imidazolidone functions. The following values were found: $\delta_d$ = 7.08, $\delta_m$ = 5.78 ppm, $K_A$ = 60 L·mol$^{-1}$ for the amide and $\delta_d$ = 5.8, $\delta_m$ = 3.7 ppm, $K_I$ = 150 L·mol$^{-1}$ for the imidazolidone N-H groups. This last value is close to those found in solution for other imidazolidone compounds.[4,5]

**Table S4.** Experimental and fitted chemical shifts as a function of total concentration of compound **S1**. Solvent is $CCl_4$ :$C_6D_6$ (90:10 v/v).

| Concentration (mmol/L) | $d_I$ (ppm) found | $d_I$ (ppm) calc. | $d_A$ (ppm) found | $d_A$ (ppm) calc |
|---|---|---|---|---|
| 0.1 | - | 3.76 | - | 5.80 |
| 0.25 | 3.83 | 3.84 | 5.83 | 5.82 |
| 0.5 | 3.93 | 3.95 | 5.88 | 5.85 |
| 1 | 4.08 | 4.11 | 5.93 | 5.91 |
| 2 | 4.30 | 4.32 | 6.00 | 6.00 |
| 3 | 4.48 | 4.46 | 6.07 | 6.07 |
| 4 | 4.58 | 4.57 | 6.12 | 6.12 |
| 5 | 4.65 | 4.65 | 6.17 | 6.17 |

## 5. TGA data of the end capping molecules

TGA was conducted for the end cap molecules as shown in Figure S6. The inset represents the curves within the weight range between 90 to 100%. From the inset, it is evident that for compounds having a primary amine end-group: compound **1** (black), compound **4** (blue), compound **5** (purple), the onset of mass decay occurs at lower temperatures than for compounds bearing an ester end-functional group : compound **2** (green), compound **3** (light blue) and a derivative of UDETA where the $NH_2$ function is acylated (red). Besides, the temperature where the weight drops below 50% of the initial mass seems more related to volatilization as it basically follows the order of increasing molecular weight (i.e., **1** < **2** < **3** < **4** < **5**).

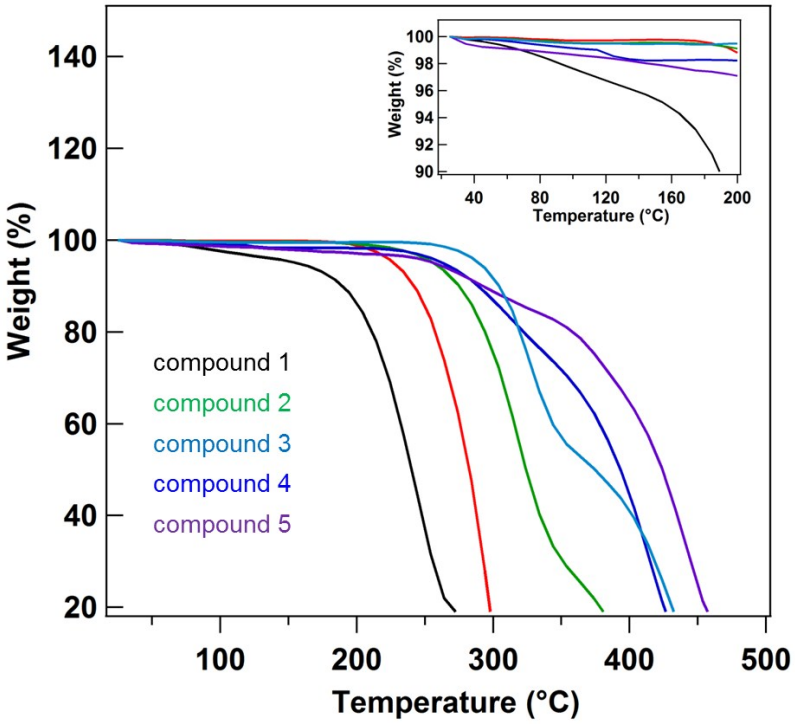


Figure S6. TGA data of end cap molecules. The colors of curves correspond with the samples in the same color. The red curve corresponds to the data of molecule synthesized by UDETA and acetic acid. The inset represents the expanded curves at initial decay of mass within the weight range between 90 to 100%.

## 6. DSC thermograms

Effects of annealing treatment on the thermograms are shown Figure S7(a). The thermograms on cooling for the annealed samples are provided in Figure S7(b). Experimental set-up and conditions are described in the experimental section of the main text.

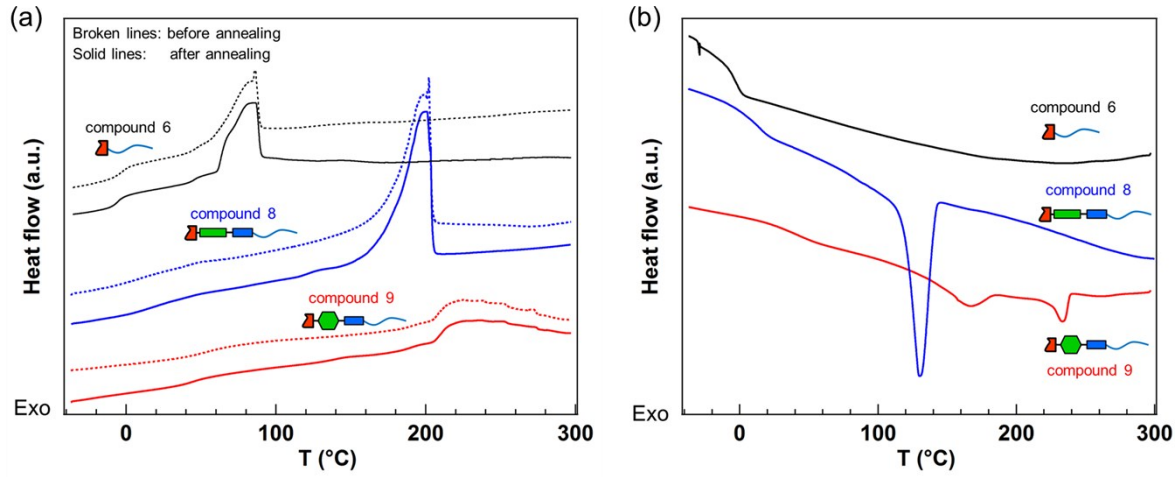


Figure S7. (a) DSC thermograms on heating for the samples before and after annealing. Broken lines represent the thermograms for the samples without annealing while solid lines indicate the ones for the samples after annealing, where the annealing was conducted at a temperature 80 ºC higher than $T_g$. (b) DSC themograms on cooling. In both (a) and (b), black, blue, and red thermograms represent the ones of compound **6**, compound **8**, and compound **9**, respectively.

## 7. Isothermal TGA data of final compounds

Isothermal TGA measurements were conducted to check the degradation progress at high temperatures. The measurement temperature corresponds to the highest temperatures experienced in rheological analyses. The measurements time was 5 hours, which was sufficiently longer time scale than that of the rheological measurements.

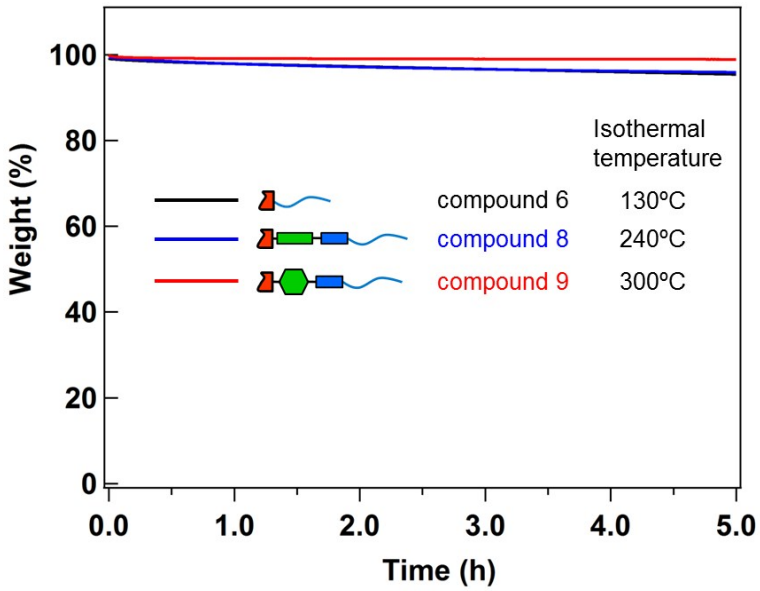


Figure S8. Isothermal TGA data of compound **6** at 130 ºC (black), compound **8** at 240 ºC (blue), and compound **9** at 300 ºC (red).

## 8. Variable temperature FT-IR measurements on compound 8 and compound 6

The changes of FT-IR spectra with an increase in temperatures for compound **8** and compound **6** are shown in Figure S9 and S10, respectively. In the similar way to the changes of compound **9** described in the main text, the positions of peaks originated from N-H and C=O vibrations dramatically change in the vicinity of the melting point whereas the position of aliphatic $CH_2$ vibrations arising from the alicyclic skeleton of Pripol 1009 is not affected by the temperature changes.

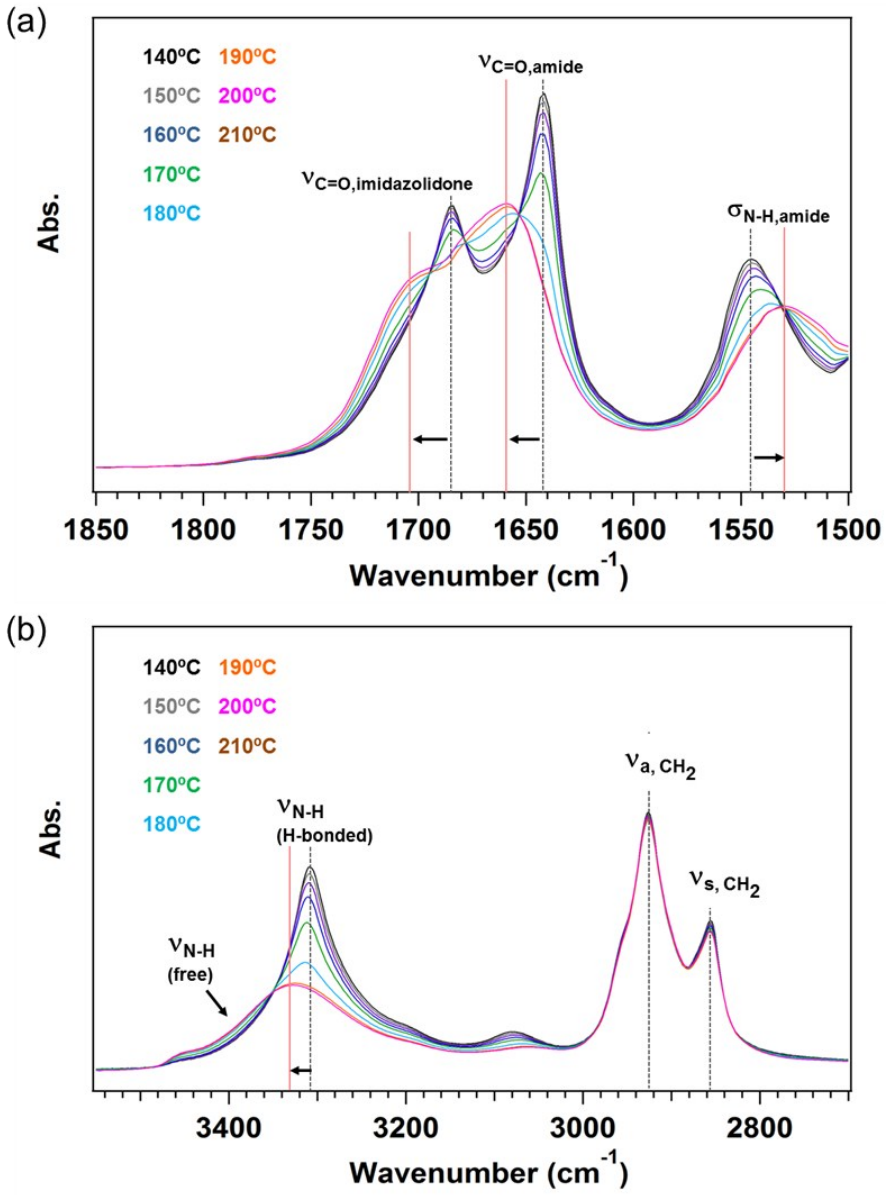


Figure S9. FT-IR spectra of compound **8** as a function of temperature (a) at the carbonyl absorption region and (b) at the high wavenumber region. The colors of spectra correspond with the measurement temperatures in the same color. In the spectra, broken black lines and red lines represent the peak positions at 140 ºC and 210 ºC, respectively, where arrows between the lines indicate the shift direction with an increase in temperatures.

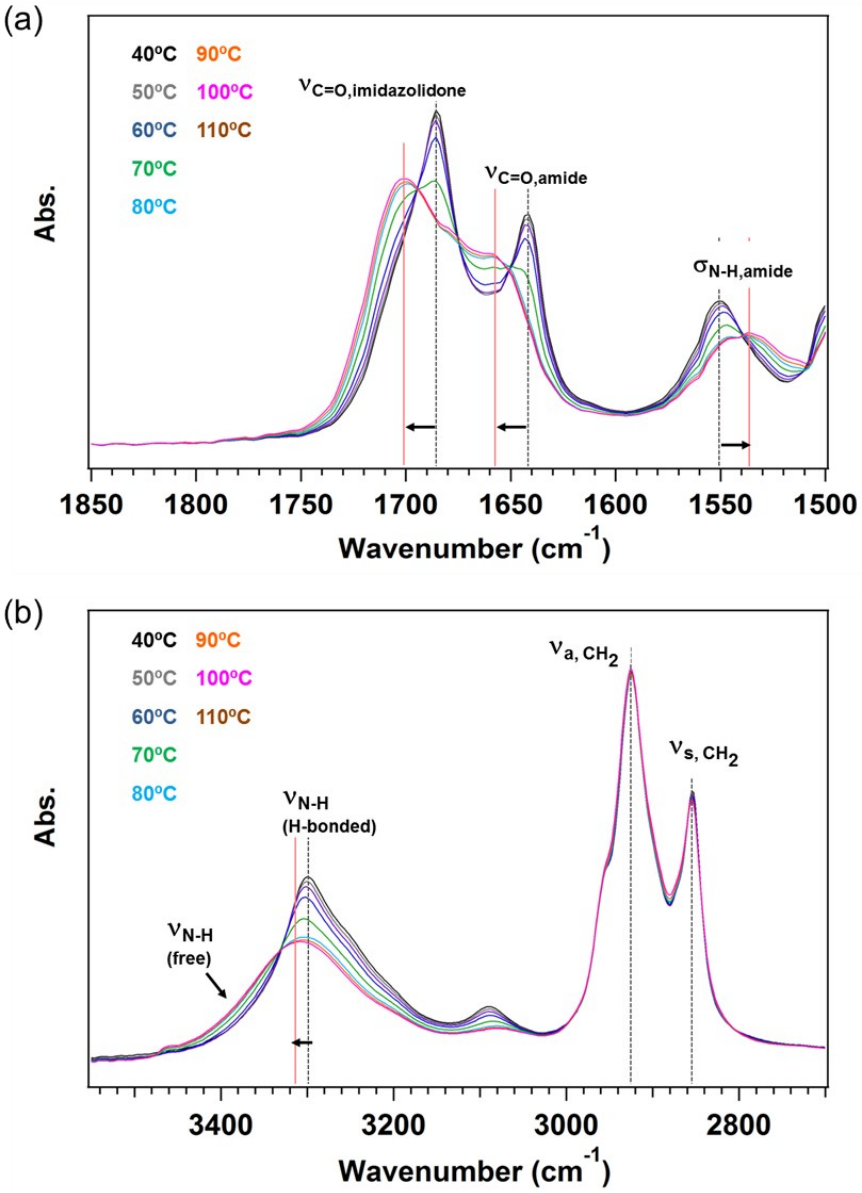


Figure S10. FT-IR spectra of compound **6** as a function of temperature at (a) the carbonyl absorption region and (b) the high wavenumber region. The colors of spectra correspond with the measurement temperatures in the same color. In the spectra, broken black lines and red lines represent the peak positions at 40 ºC and 110 ºC, respectively, where arrows between the lines indicate the shift direction with an increase in temperatures.

## 9. Plots of $\ln\eta$ as a function of inverse temperatures

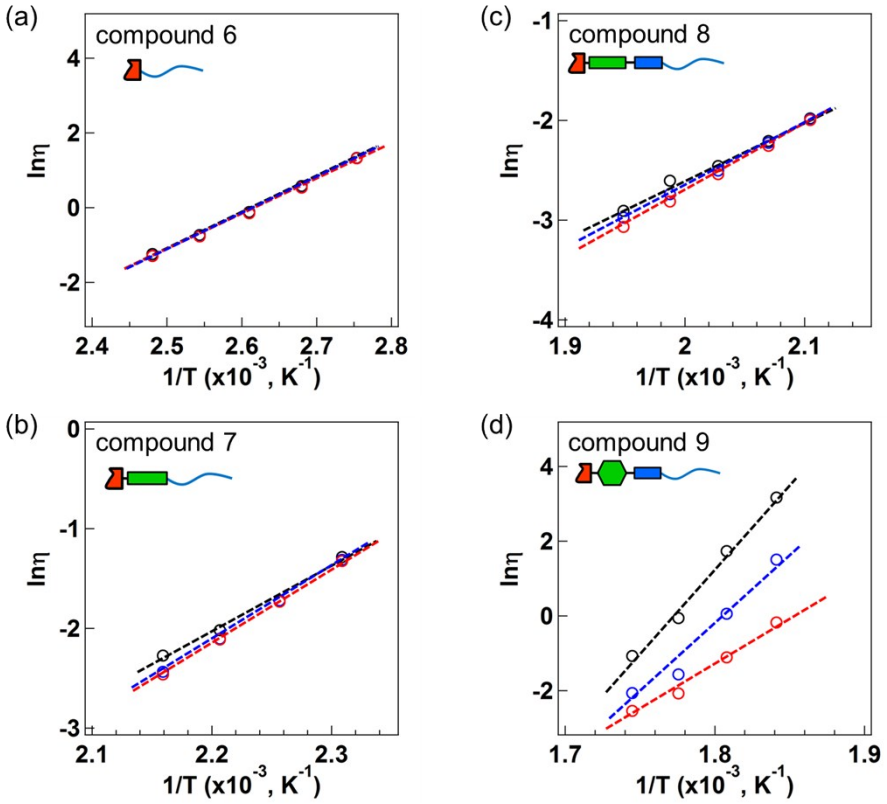


Figure S11. Plots of $\ln\eta$ as a function of inverse temperatures: (a) compound **6**; (b) compound **7**; (c) compound **8**; (d) compound **9**. The plots were made at three shear rates; 1.56 $s^{-1}$ (black), 14.1 $s^{-1}$ (blue), 129 $s^{-1}$ (red). For compound **9**, the plots were based on the data obtained by the measurements from low shear rate.

## 10. Tensile data of compound 6

Tensile tests were performed on compound **6**, using dog-bone shaped samples. To this end, rectangular plates of 1.4 mm thickness were prepared by pressing the molten material in a brass frame sandwitched between two non-adhesive paper sheets. After slow cooling down to room temperature, dogbone specimens of ISO 527-3 shape with working dimensions of 20 mm × 4 mm were cut using a heated punch. Tensile tests were performed at room temperature using an Instron Universal Tester Model 5565 with a load cell of 100 N at a stretching rate of 2 mm / min. The obtained curve is shown in Figure S12a. At room temperature, compound **6** shows a Young modulus of about 25 ( ± 5) MPa, an elongation at break of about 10%, and the stress at break of about 2 MPa. The tensile test also revealed the occurence of the necking phenomenon, as shown in figure S12b.

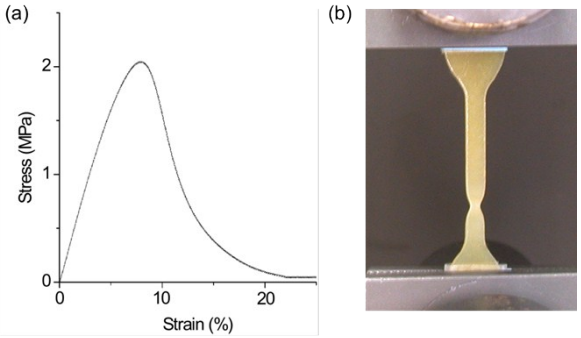


Figure S12. (a) Stress-strain curve obtained for compound **6** and (b) macroscopic image of the sample during the measurement.

## 11. References


[1] R. Agnaou, M. Capelot, S. Tencé-Girault, F. Tournilhac and L. Leibler, *J. Am. Chem. Soc.,* 2014, **136**, 11268.

[2] A. M. Aerdts, K. L. L. Eersels, and G. Groeninckx *Macromolecules,* 1996, **29**, 1041.

[3] D. B. Davies, S. F. Baranovsky, A. N. Veselkov, *J. Chem. Soc., Faraday Trans*. 1997, **93**, 1559.

[4] E. Gentric, J. Lauransan, C. Roussel, F. A. Devillanova, G. Verani, J. *Heterocyclic Chem.* 1979, **16**, 1083.

[5] D.W. Johnson, L.C. Palmer, T. Martin, U. Obst, J.J. Rebek, *Chem. Commun.*, 2003, **14**, 1638.